

Density Profiles in Seyfert Outflows

Ehud Behar^{1,2}

ABSTRACT

For the past decade, ionized outflows of a few 100 km s⁻¹ from nearby Seyfert galaxies have been studied in great detail using high resolution X-ray absorption spectra. A recurring feature of these outflows is their broad ionization distribution including essentially ions (e.g., of Fe) from neutral to fully ionized. The absorption measure distribution (*AMD*) is defined as the distribution of column density with ionization parameter $|dN_H/d(\log \xi)|$. *AMDs* of Seyfert outflows can span up to five orders of magnitude in ξ . We present the *AMD* of five outflows and show that they are all rather flat, perhaps slightly rising towards high ionization. More quantitatively, a power-law fit for $\log AMD \propto (\log \xi)^a$ yields slopes of $0 < a < 0.4$. These slopes tightly constrain the density profiles of the wind, which until now could be addressed only by theory. If the wind is distributed on large scales, the measured slopes imply a generic density radial profile of $n \propto r^{-\alpha}$ with $1 < \alpha < 1.3$. This scaling rules out a mass conserving radial flow of $n \propto r^{-2}$, or a constant density absorber, but is consistent with a non-spherical MHD outflow model in which $n \propto r^{-1}$ along any given line of sight. On the other hand, if ionization variations are a result of local (δr) density gradients, e.g. as in the turbulent interstellar medium (ISM), the *AMD* slopes imply density scaling of $n \propto \delta r^{-\alpha}$ with $0.7 < \alpha < 1.0$, which is quite different from the scaling of approximately $n \propto \delta r^{0.4}$ found in the Milky Way ISM and typical of incompressible turbulence.

Subject headings: X-rays: galaxies — galaxies: active — galaxies: individual (IRAS 13349+2438, NGC 3783, NGC 7469, NGC 5548, MCG -6-30-15) — techniques: spectroscopic — galaxies: ISM

¹Senior NPP Fellow, NASA / Goddard Space Flight Center, Greenbelt MD 20771.
behar@milkyway.gsfc.nasa.gov

²Permanent address: Department of Physics, Technion, Haifa 32000, Israel.

1. INTRODUCTION

The X-ray spectra of many active galactic nuclei (AGNs) viewed directly toward the central source (e.g., Seyfert 1 galaxies) show the continuum flux absorbed by numerous absorption lines produced by ionized gas. The role of these absorbers for the AGN and for the host galaxy are still being debated. In order to advance our understanding of these outflows and their significance to the AGN, it is important to develop model-independent techniques for quantifying the physical parameters of the wind. So far, only the wind velocity measured from Doppler shifts and the total column density N_H deduced from the equivalent widths of absorption lines are known with high confidence. The broad range of ionization (and temperature) in the wind is also unambiguous. Conversely, there is little robust constraints on the location, geometry, and density of the wind, which leaves its mass outflow rate, momentum, and energy fairly uncertain.

The X-ray band can potentially provide the full physical picture of AGN outflows, as it comprises detectable absorption lines from the full range of charge states: From neutral up to hydrogen-like. The detection of all of the absorbing charge states of a given element enables an accurate measurement of the total column density. For this purpose, Fe ions are particularly useful as they form over several orders of magnitude of ionization parameter ξ

$$\xi = \frac{L}{nr^2} \quad (1)$$

where L is the ionizing luminosity between 1 and 1000 Rydberg, n denotes the hydrogen number density and r is the distance of the absorber from the ionizing source. AGN outflows can be distributed over the full range of ionization $-1 < \log \xi < 4$ (Steenbrugge et al. 2003, 2005; Costantini et al. 2007; Holczer et al. 2007). In order to best quantify this distribution, Holczer et al. (2007) defined an absorption measure distribution (*AMD*), which is the distribution of the hydrogen column density N_H along the line of sight as a function of $\log \xi$

$$AMD = |dN_H/d(\log \xi)| \quad (2)$$

Reciprocally, the total N_H can be expressed as an integral over the *AMD*. The *AMD* is the absorption analog of the Emission Measure Distribution (*EMD*) widely used in the analysis of emission-line spectra. It provides a more complete representation of the ionization distribution than the more commonly used models of several ionization components each with a fixed ξ ; the overall success of the latter in producing good spectral fits to the data notwithstanding. The *AMD* reconstruction method is outlined in detail in Holczer et al. (2007). Here, we only note that for each target, the observed continuum spectrum is used to

obtain the ionization balance as a function of ξ from the XSTAR code (Kallman & Bautista 2001). Subsequently, the *AMD* is obtained by a fitting process that aims to best reproduce all of the individually measured ionic column densities. Being the solution of an inversion problem, the reconstructed *AMD* is inevitably degenerate. Nonetheless, a step function is the preferred *AMD* form, as it allows rigorous local error calculations that take into account the degeneracy between different ξ bins. For more details see Holczer et al. (2007).

In this paper, we present the available *AMD* distributions, which were derived for five sources with high signal-to-noise-ratio X-ray grating spectra. The objective is not to focus on any individual target, but to seek trends in the best available (yet admittedly small and incomplete) sample of AGN outflows. The idea is to link the general *AMD* behavior with the physical properties of the outflows, in particular the density profile, in order to obtain an insight into the origin and astrophysical significance of the winds. These physical implications are described in §3 and discussed in §4

2. Targets and *AMD*s

We include all the Seyfert outflow targets with sufficiently good grating spectra for which we were able to reconstruct a non-degenerate *AMD*. The *AMD*s of IRAS 13349+2438 and of NGC 3783 were presented in great detail in Holczer et al. (2007) and are based on deep exposures with the HETGS spectrometer on board *Chandra*. The *AMD* of MCG –6–30–15 is from a recent analysis of the HETGS spectrum (Holczer et al., in preparation) and corresponds to the slow AGN component in that complex spectrum. The *AMD* of NGC 5548 was derived from the ionic column densities published by Steenbrugge et al. (2005) and based on spectra from the HETGS and LETG instruments on board *Chandra*. The *AMD* of NGC 7469 is an improved version of that presented in Blustin et al. (2007) and is based on spectra acquired with the RGS spectrometer on board *XMM-Newton*. The improvement is that unlike in Blustin et al. (2007), here we followed the general method of Holczer et al. (2007) and allowed the *AMD* to be zero in certain bins, if required by the fit. We note that a thorough spectral analysis was carried out also for the *Chandra* LETG spectrum of Mrk 279 by Costantini et al. (2007). However, the low column density and marginal detection of Fe absorption in Mrk 279 is insufficient to produce a well constrained *AMD*.

The five *AMD*s used in the present work are plotted in Fig. 1. Note that all *AMD*s have a gap at intermediate ξ values, which is in fact a data point at zero that is not plotted. For four sources this gap falls between $\log \xi \approx 0.5 - 1.5$ erg s⁻¹ cm, while for NGC 7469 it is at slightly higher values. In Holczer et al. (2007) and in Blustin et al. (2007), these *AMD* discontinuities were interpreted as regions of thermal instability. A physically separated two-

component outflow is another possible interpretation, although the similar outflow velocities of the low and high ionization regions and the ubiquity of the minimum at approximately the same temperature regime argue against two separate components. The presence of the thermally unstable region and its exact position (in ξ) depend strongly on the correspondence between charge state and ξ that are derived from XSTAR (Kallman & Bautista 2001) and are uncertain to some degree. It is known, for instance, that some of the available dielectronic recombination (DR) rates used in these computations are inadequate (Netzer 2004; Badnell 2006). Another effect that could potentially change the unstable region by affecting the ξ at which low charge states form in the outflow is photoionization of these ions by the EUV continuum that is poorly constrained. Finally, all ionization balance computations are carried out with a single ionizing spectrum, i.e., in the optically thin limit. This is justified by the observed X-ray spectra that typically show only shallow photoelectric edges, if any. Once the medium becomes optically thick and deeper regions are exposed to lower (and harder) ionizing luminosity, this approximation gradually loses its validity.

In this work, we are interested more in the broad characteristics of the distribution. Assuming that the minimum is due to thermal instability justifies viewing the remaining stable regions of the *AMD* as different ionization components of the same outflow that are likely driven by the same physical mechanisms. We thus apply simple (least mean square) linear fits to each *AMD* according to $\log AMD(\xi) = a \log \xi + b$, or $AMD(\xi) = 10^b \xi^a$. The allegedly thermally unstable ionization regions are ignored in the fit. A similar power law distribution of ionization was suggested by Steenbrugge et al. (2003). It can be seen in Fig. 1 that a power law representation of the *AMD* for some targets is far from perfect. Nevertheless, given the uncertainties on each data point, and for the mere purpose of seeking *AMD* trends, we deem it sufficient. Moreover, a power law *AMD* representation allows direct comparisons with self-similar wind models as discussed in the following sections. The best-fit power laws for the five outflows are shown in Fig. 1 and the fit parameters are listed in Table 1. Evidently, all five power laws have relatively similar slopes of $a = 0.0 - 0.4$. The implied density profile slopes (α), introduced in the next section, are also listed in Table 1. Steenbrugge et al. (2005) fitted a power law to their distribution of individual ionic column densities in NGC 5548, which is somewhat similar but not identical to the full *AMD* (see Holczer et al. 2007, for details). They obtained a slope of $a = 0.2 \pm 0.1$ (denoted there α) with Fe ions alone, which is in excellent agreement with our best-fit of $a = 0.14 \pm 0.08$. When they use other elements, however, and need to rely on the assumption of solar abundances, they get a somewhat steeper slope of $a = 0.4$.

3. Physical Implications for Outflows

In this section, we explore what the *AMD* shape, namely its slope, implies for the density profile of the outflow. It is convenient for this purpose to consider two separate boundary cases. One is a radial large-scale outflow in which the density $n(r)$ varies as a function of the distance from the source r . In this case, $\xi = L/(nr^2)$ varies along the flow due to the combined change in r and in n . The other possibility is a remote absorber at a distance more or less constant $r = r_0$, but with strong density gradients over small distances $\delta r \ll r_0$. In this case, the ionization varies exclusively due to the local density gradients. Obviously, a real outflow could be a combination of the two, namely a large scale outflow with strong local density gradients. However, for the current analysis, it is instructive to consider these two cases separately.

3.1. Large Scale Outflow

A large-scale outflow is defined here as an outflow with a size comparable to the distance r from the ionizing source so that the ionization parameter (eq. 1) is a function of r also through the parameterization of $n(r)$. Let us assume a power-law density profile with an index $\alpha > 0$

$$n(r) \propto r^{-\alpha} \quad (3)$$

Such a parameterization of the density is convenient for comparison with self-similar wind solutions. The ionization parameter thus varies with radius as $\xi(r) \propto r^{\alpha-2}$, or reciprocally $r(\xi) \propto \xi^{1/(\alpha-2)}$ and

$$\frac{dr}{d\xi} \propto \xi^{-\frac{\alpha-3}{\alpha-2}} \quad (4)$$

The radial increment of hydrogen column density N_H with the ionization parameter $\xi(r)$, can be written as

$$dN_H \equiv n(r)dr = n(r)\frac{dr}{d\xi}d\xi \propto \xi^{-\frac{2\alpha-3}{\alpha-2}}d\xi \quad (5)$$

Consequently, the *AMD* (eq. 2) scales with ξ as

$$AMD = \left| \frac{dN_H}{d \log \xi} \right| \propto \xi \left| \frac{dN_H}{d\xi} \right| \propto \xi^{-\frac{\alpha-1}{\alpha-2}} \equiv \xi^a \quad (6)$$

where $a = -(\alpha - 1)/(\alpha - 2)$ is precisely the slope of $\log AMD$ vs. $\log \xi$ fitted for in Fig. 1. Finally, α and its uncertainty can be expressed as

$$\alpha = \frac{1 + 2a}{1 + a} \pm \frac{\Delta a}{(1 + a)^2} \quad (7)$$

where Δa stands for the standard error of the fitted power law slope a . The resulting α values for the five outflows are listed in Table 1. Note that a scaling with ξ similar to that of eq. (6) is obtained for the integrated N_H up to r , as $N_H(r) \propto \int_0^r n(r') dr' \propto r^{1-\alpha} \propto \xi^{-\frac{\alpha-1}{\alpha-2}}$. However, $N_H(r)$ is a property that pertains to the entire flow up to radius r , while the AMD is a local property of the flow at each position (or as a function of ξ), and is therefore preferred here.

Note that for AMD s that increase with ξ (i.e., flow dominated by high charge states) as found in the present sample, α must obtain values between 1 – 2. The observed slopes, e.g., of $a = 0, 0.25, \text{ or } 0.4$, imply density profiles that are not particularly steep with respective indices of $\alpha = 1.0, 1.2, \text{ and } 1.3$. A steep AMD over *narrow* ranges of ξ , on the other hand, is difficult to rule out. Indeed, by inspecting Fig. 1, it can be seen that some outflows (e.g., NGC 3783, MCG–6–30–15, NGC 5548) tentatively show steeper AMD s at low ionization (ξ) that flatten out at higher ξ . By analyzing eq. (6), a few special cases can be easily examined.

For a *constant-density* n_0 absorber, $\alpha = 0$, and the AMD would slowly decrease with ionization parameter as $AMD(n_0) \propto \xi^{-1/2}$. No slope with $a < 0$ is observed in the five present outflows, which rules out a constant density outflow. Indeed, the constant density scenario is quite unphysical.

Yet another possible wind scenario is a steady mass conserving radial flow similar to a stellar wind, in which the mass outflow rate, opening angle, and wind velocity are all constant. This results in a density profile $n \propto r^{-2}$, or $\alpha = 2$. Such a flow was assumed for instance by Krolik & Kriss (1995). In terms of the AMD slope a , it tends to infinity (eq. 6). In this case, the ionization parameter would of course be constant (ξ_0) along the flow implying a sharply peaked AMD (around ξ_0). This is in stark contradiction with the present sample that all feature broad AMD s. It is worth noting however, that some Seyferts do show distinctly faster (few 1000 km s⁻¹) and more highly-ionized ($\log \xi > 3$) outflows that perhaps could be characterized by a single ionization parameter, a good example of which is the high-velocity components (4500 km s⁻¹ & 1900 km s⁻¹, respectively) found

in NGC 4051 (Steenbrugge et al. 2009) and in MCG –6–30–15 (Sako et al. 2003). The low and intermediate charge states are clearly absent from these high-velocity components that do not have the same broad AMD as the present, slower winds. This along with the lack of a continuous velocity distribution (c.f., distinct slow and fast components) suggests that the slow and fast outflows are different types of winds, and may also differ in their position within the AGN system.

All of the outflows observed to date for which an AMD could be reconstructed imply a flat to modestly *increasing* AMD with ξ . The column density measured for the low-ionization species is generally never higher than that of the high ionization plasma in terms of equivalent N_H . In order to obtain a strictly flat AMD while retaining the assumption of a global power-law density dependence on radius (eq. 3), the density scaling must obey $n(r) \propto 1/r$ (or $\alpha = 1$). Allowing for a moderately increasing AMD with ξ , as observed in Fig. 1 results in density scalings $r^{-\alpha}$ with $1 < \alpha < 1.3$. See Table 1 for details.

3.2. Small Scale Outflow

Perhaps an equally interesting case is a distant absorber (at r_0) in which the ionization parameter distribution $\xi \approx L/(nr_0^2)$ is driven by density gradients on much smaller distances ($\delta r \ll r_0$). The broad AMD then requires the density to vary by several orders of magnitude to account for the different orders of magnitude of observed ξ . Such a multi-phase scenario could be a natural consequence, e.g., of turbulence as observed in the interstellar medium (ISM) gas in our galaxy. Indeed, such a description for Seyfert outflows was proposed by Chelouche & Netzer (2005) for NGC 3783 and further systematically explored for similar outflows in Chelouche (2008).

We now assume the density varies locally on these small length scales δr

$$n(\delta r) \propto \delta r^{-\alpha}, \quad (8)$$

which merely reflects typical density variations with distance that are assumed to be isotropic. In this case, the dependence of the AMD on α is slightly different than in Eqs. (4 - 6), as $\xi \propto n^{-1} \propto \delta r^\alpha$, subsequently $\frac{d(\delta r)}{d\xi} \propto \xi^{-\frac{\alpha-1}{\alpha}}$, $dN_H = n(\delta r)\frac{d(\delta r)}{d\xi}d\xi \propto \xi^{-\frac{2\alpha-1}{\alpha}}d\xi$, and the AMD scales with ξ as

$$AMD(r = r_0) = \left| \frac{dN_H}{d \log \xi} \right| \propto \xi \left| \frac{dN_H}{d\xi} \right| \propto \xi^{-\frac{\alpha-1}{\alpha}} \equiv \xi^a \quad (9)$$

where again a is the *AMD* slope and thus here $a(r = r_0) = -(\alpha - 1)/\alpha$, and inversely

$$\alpha = \frac{1}{1 + a} \pm \frac{\Delta a}{(1 + a)^2} \quad (10)$$

which can be compared with the large-scale flow relation given in eq. (7). Here again, Δa is the standard error of the fitted power law slope a . The resulting values for the five outflows considered here are listed in Table 1. The functional forms of the density scaling α in eqs. (7) and (10) are generally different. However, in the relevant regime of observed slopes $a \approx 0$ (and only there), the value of α implied by both expressions is similar and close to unity. We obtain $1 < \alpha < 1.3$ for the large scale flows and $0.7 < \alpha < 1$ for the small scale (constant r_0) flows. Far from $a = 0$, the two would be significantly different.

It has been shown by Gonçalves et al. (2006) that strong density gradients can occur naturally in an absorbing slab that is in pressure balance as thermal instabilities (suggested also by the discontinuous *AMDs* in Holczer et al. 2007) result in strong temperature jumps that in turn cause strong density gradients. Chelouche & Netzer (2005) propose a different model for NGC 3783 of thermal launching of a wind with assumed strong density gradients on small length scales and invoke a density scaling similar to eq. (8). They obtained a density profile with $\alpha = 0.8$ (denoted there as $-\beta$), which is in very good agreement with the present results. Chelouche (2008) recently applied the same model to a sample of outflows. However, the values quoted in Chelouche (2008) are $\alpha \approx 1.3 \pm 0.6$, systematically higher than what we find here, although still consistent given their large errors. In any event, the present method provides much tighter constraints on α (Table 1).

4. Discussion

The *AMD* slope defined in Eqs. (6) and (9) provides a novel way to obtain a self similar density profile of the outflow. The slopes available for a handful of outflows are all quite similar and lie in the range of $0 < a < 0.4$. The fact that a is not much larger than zero reflects the broad and relatively flat ionization distribution of Seyfert outflows. Along with the moderate velocities of a few 100 km s^{-1} , these are the only two model-independent recurring features of such flows. In §3, we quite generally differentiate between two possible physical flows that could produce this *AMD* profile. One is a large scale AGN outflow that would need to have a density profile of $n \propto r^{-\alpha}$ with power-law indices of $1 < \alpha < 1.3$ in order to reproduce the observed *AMD*. Importantly, a smooth radial mass conserving flow of $n \propto r^{-2}$, for example, that would correspond to a single ξ or a sharply peaked *AMD* are conclusively ruled out, and so is a constant-density absorber ($a = -0.5$). Another possibility

is a remote absorber with strong density gradients on local length scales δr in which case $n \propto \delta r^{-\alpha}$ and $0.7 < \alpha < 1$.

If the outflow originates in the accretion disk, as believed by many authors, it is of the large scale type. The derived density profiles can thus be compared directly with an entire family of self-similar solutions for hydromagnetic (MHD) disk winds (Contopoulos & Lovelace 1994). To obtain an MHD wind with a slope of $\alpha = 1.5$, for example, as in Blandford & Payne (1982) would require a *global AMD* slope of $a = 1.0$ that is clearly excluded by the data. Such a high index is not seen in any of the Seyfert outflows (Fig. 1, Table 1). Models from Contopoulos & Lovelace (1994), on the other hand, with $1 < \alpha < 1.3$ are consistent with the observed *AMDs* (the present α corresponds in their notation to $3 - 2x$). In fact, the specific self-similar solution with $\alpha = 1$ was preferred by Königl & Kartje (1994) for its minimal magnetic energy. It is interesting to note that a totally different approach using the temporal behavior of accreting sources suggests indices of $\alpha = 1 - 1.5$ for the Compton scattering medium that produces the continuum X-ray spectrum (Kazanas et al. 1997; Hua & Kazanas 1997). Consequently, a detailed MHD wind model has been developed by Fukumura et al. (in preparation) with an $n \propto r^{-1}$ profile that by definition produces a flat *AMD*. Note that density profiles that significantly deviate from $n \propto r^{-2}$ have been reported out to the narrow line region (NLR). Bennert et al. (2006) measured values of $\alpha = 1.46 \pm 0.2$ and $\alpha = 1.14 \pm 0.1$, respectively, for a sample of Seyfert 1 and Seyfert 2 NLRs.

For local density gradients, it is instructive to think of pressure-balanced clouds. This type of models uses an absorbing slab to represent the AGN outflow, and with careful numerical treatment of the radiative transfer problem through the slab can compute its temperature, density, and ionization distributions (Gonçalves et al. 2006). The astrophysical context of such "slabs" and how they are launched remains to be sorted out, but models such as those of Gonçalves et al. (2006) already stand out by virtue of their continuous and broad *AMD*, which is observed for Seyfert outflows. In fact, with some fine tuning, these models can reproduce the majority of the measured ionic column densities, as well as the observed unstable region of the *AMD*. On the other hand, they also predict other unstable regions that are not necessarily observed as such. The numerical nature of these radiative transfer codes does not straightforwardly provide for an analytical power law density profile to be directly compared with eqs. (8) and (10).

An alternative natural source of density gradients on many scales is turbulence, such as that found in the interstellar medium (ISM) of the Milky Way. For a recent review of ISM observations and the relevant physical processes, see Elmegreen & Scalo (2004). A general feature of the ISM is its power spectrum

$$P(k) \propto k^{-p} \quad (11)$$

observed to be approximately a power law over five decades in wavenumber $k = 1/\delta r$ from $10^{-15} - 10^{-10} \text{ cm}^{-1}$ (Armstrong et al. 1995). The standard definitions are used here for $P(k) \equiv \hat{n}(k)\hat{n}(k)^*$ where $\hat{n}(k)$ is the Fourier transform of an observable quantity (e.g., density) $n(\delta r)$, and $\hat{n}(k)^*$ is its complex conjugate. Typically, 3D ISM power spectra are consistent with, or slightly steeper than the Kolmogorov spectrum for non-magnetic, incompressible turbulence in which $p = 11/3$, as a result of energy cascading from large to small scales with no preferred intermediate scale (Kolmogorov 1941). Somewhat steeper power spectra ($p = 4$) can be expected from random shocks (Saffman 1971). While in a magnetic, compressible turbulent medium, density fluctuations can scale differently on different length scales (Lithwick & Goldreich 2001), the prevalent spectrum over most scales is a Kolmogorov one. Hence, for the most part a value of $p = 3.8 \pm 0.2$ is a reasonable approximation for the ISM.

In order to obtain a density scaling akin to eq. (8) for turbulent media, the mean squared density variations (variance) can be estimated from the volume 3D integral in Fourier space of the power spectrum (Parseval’s theorem) over a cell the size of $1/\delta r$

$$\langle |\delta n^2| \rangle = \int P(k) d^3k \propto \delta r^{p-3} \quad (12)$$

The root mean square (rms) of the density fluctuations in a volume $\sim \delta r^3$ thus scales as

$$\delta n_{\text{rms}}(\delta r) = \sqrt{\langle |\delta n^2| \rangle} \propto \delta r^{\frac{p-3}{2}} \quad (13)$$

If this rms of density fluctuations is understood as the typical scaling of density variations over δr as in $n(\delta r) \propto \delta r^{-\alpha}$ with $\alpha = (3-p)/2$, it can be directly compared with eq. (8). Note that since generally $p > 3$, the density fluctuations do not vanish at any scale within the medium (i.e., no asymptotic homogeneity). Thus, eq. (13), in principle, could be meaningful over many orders of magnitude.

Applying the typical ISM value of $p = 3.8 \pm 0.2$ yields a density scaling of $n \propto \delta r^{0.4}$ ($\alpha = -0.4 \pm 0.1$). Recall that using the *AMD* slopes, we obtained markedly different density gradients with $0.7 < \alpha < 1.0$ (Table 1). Another difference between the Seyfert outflow and typical ISM is the range in density. For a distant, localized (r_0) Seyfert absorber, the range in density required for producing the observed ionization structure needs to span up to five orders of magnitude ($-1 < \log \xi < 4$). It is not clear that the ISM spans such a broad density

range, and certainly not within a single medium (e.g., a molecular cloud). The observed five orders of magnitude in k in the ISM correspond to only ($n \propto k^{-0.4}$) two orders of magnitude in density. In order to obtain the high density gradients of $0.7 < \alpha < 1.0$, an extremely shallow power spectrum with $p = 0.8 - 1.0$ would be required. We are not aware of any other (ISM) medium with such a flat power spectrum.

5. CONCLUSIONS

We have presented the Absorption Measure Distribution (*AMD*) of five nearby AGN outflows. The *AMD* is the differential column density through the flow as a function of ionization parameter ξ that can be derived from the high resolution X-ray absorption spectrum of the outflow. Key to reconstructing the *AMD*s is the observation of almost all Fe charge states from neutral to H-like. Using a power law approximation, we fit for the *AMD* slopes and find that there is only a mild increase of column density with ξ , namely the slopes are all in the range of 0 to 0.4. It may be possible that at low ionization $\log \xi < 1$, the *AMD* is steeper and then flattens out towards higher ionization ($\log \xi > 2$). However, the limited ionization resolution in the *AMD* (due to the large formation regions of the various charge states) does not allow for a more precise assessment. In any event, the *AMD* reconstruction at low ionization is currently hampered by the uncertain dielectronic recombination rates and by the unknown EUV continuum. We expect the former limitation to be remedied soon by new laboratory measurements and improved atomic calculations. We also expect more high-quality grating spectra of AGN outflows to be released to the *Chandra* and *XMM-Newton* archives in the next few years. Future high throughput X-ray spectrometers, such as the SXS currently being built for *Astro-H* will further increase the sample. As the sample of well studied Seyfert outflows increases, the present method will continue to facilitate our growing understanding of the physics governing these winds.

We have discussed the best-fit *AMD* slopes in the context of two qualitatively different scenarios, one is a continuous large-scale radial flow and the other is a distant well localized absorber. If the outflow is of the former type, we can constrain its density profile rather tightly to $n \propto r^{-\alpha}$ with $1 < \alpha < 1.3$. This already rules out the standardly assumed $n \propto r^{-2}$ profile, or even a profile of $n \propto r^{-1.5}$. A constant-density absorber ($\alpha = 0$) is also clearly ruled out. An MHD wind, on the other hand, with a shallower density profile of $\alpha \gtrsim 1$ as proposed by Fukumura et al. (in preparation) is consistent with the observed outflows. Alternatively, slab models with proper radiative transfer can produce a broad ionization distribution, with intermediate thermally unstable regions, generally consistent with the observed *AMD*s. If the absorber is remote from the central source, and compact, then its ionization depends

solely on the local density gradients. We find that in this case, the density should vary as $n \propto \delta r^{-\alpha}$ with $0.7 < \alpha < 1$. Such sharp gradients, and occurring over five orders of magnitude in density, are quite different from those typically found in the Milky Way ISM and interpreted as due to turbulence.

I thank Tomer Holczer for providing the *AMD* results in simple data form and Alex Blustin for suggesting the title for the paper.

REFERENCES

- Armstrong, J. W., Rickett B. J., & Spangler, B. 1995. *ApJ*, 443, 209
- Badnell, N. R. 2006, *ApJ*, 651, L73
- Bennert, N., Jungwiert, B., Komossa, S., Haas, M., & Chini, R. 2006, *A&A*, 459, 55
- Blandford, R. D. & Payne D. 1982, *MNRAS*, 199, 883
- Blustin, A. J., et al. 2007, *A&A*, 466, 107
- Chelouche, D. & Netzer, H. 2005, *ApJ*, 625, 95
- Chelouche, D., unpublished astro-ph/0812.3621
- Contopoulos, J. & Lovelace, R. V. E. 1994, *ApJ*, 429, 139
- Costantini et al. 2007, *A&A*, 461, 121
- Crenshaw, D. M., Kraemer, S. B., George, I. M., 2003, *ARA&A*, 41, 117
- Elmegreen, B. G. & Scalo, J. 2004, *ARA&A*, 42, 211
- Gonçalves, A. C., Collin, S., Dumont, A.-M., Mouchet, M., Rozanska, A., Chevallier, L., & Goosmann, R. W. 2006, *A&A*, 451, L23
- Holczer, T., Behar, E., & Kaspi, S. 2007, *ApJ*, 663, 799
- Hua, X.-M. & Kazanas, D. 1997, *ApJ*, 482, L57
- Kallman, T. R. & Bautista, M. 2001, *ApJS*, 133, 221
- Kazanas, D., Hua, X.-M. & Titrachuk, L. 1997, *ApJ*, 480, 735
- Kolmogorov, A. 1941, *Dokl. Akad. Nauk SSSR*, 31, 538
- Königl A. & Kartje, A. F. 1994, *ApJ*, 434, 446
- Krolik, J. H. & Kriss, G. A. 1995, *ApJ*, 447, 512
- Lithwick Y. & Goldreich P. 2001, *ApJ*, 562, 279
- Netzer, H. 2004, *ApJ*, 604, 551
- Saffman, P. G. 1971, *Stud. Appl. Math.* 50, 377

Sako, M. et al. 2003, ApJ, 596, 114

Steenbrugge, K. C., Kaastra, J. L., de Vries, C. P., & Edelson, R. 2003, A&A, 402, 477

Steenbrugge, K. C. et al. 2005, A&A, 434, 569

Steenbrugge, K. C. et al. 2009, A&A, 496, 107

Table 1. Best-fit parameters from the linear fits in Fig. 1 $AMD(\xi) \propto \xi^a$

Target	Slope (a)	α^a	α^b
NGC 3783	0.29 ± 0.11	1.22 ± 0.07	0.78 ± 0.07
IRAS 13349+2438	0.02 ± 0.01	1.02 ± 0.01	0.98 ± 0.01
MCG –6–30–15	0.10 ± 0.11	1.10 ± 0.09	0.91 ± 0.09
NGC 5548	0.14 ± 0.08	1.12 ± 0.06	0.88 ± 0.06
NGC 7469	0.24 ± 0.13	1.19 ± 0.08	0.80 ± 0.08

^aFor a distance driven AMD , $\alpha = (1 + 2a)/(1 + a)$, as in §3.1

^bFor a density driven AMD , $\alpha = 1/(1 + a)$, as in §3.2

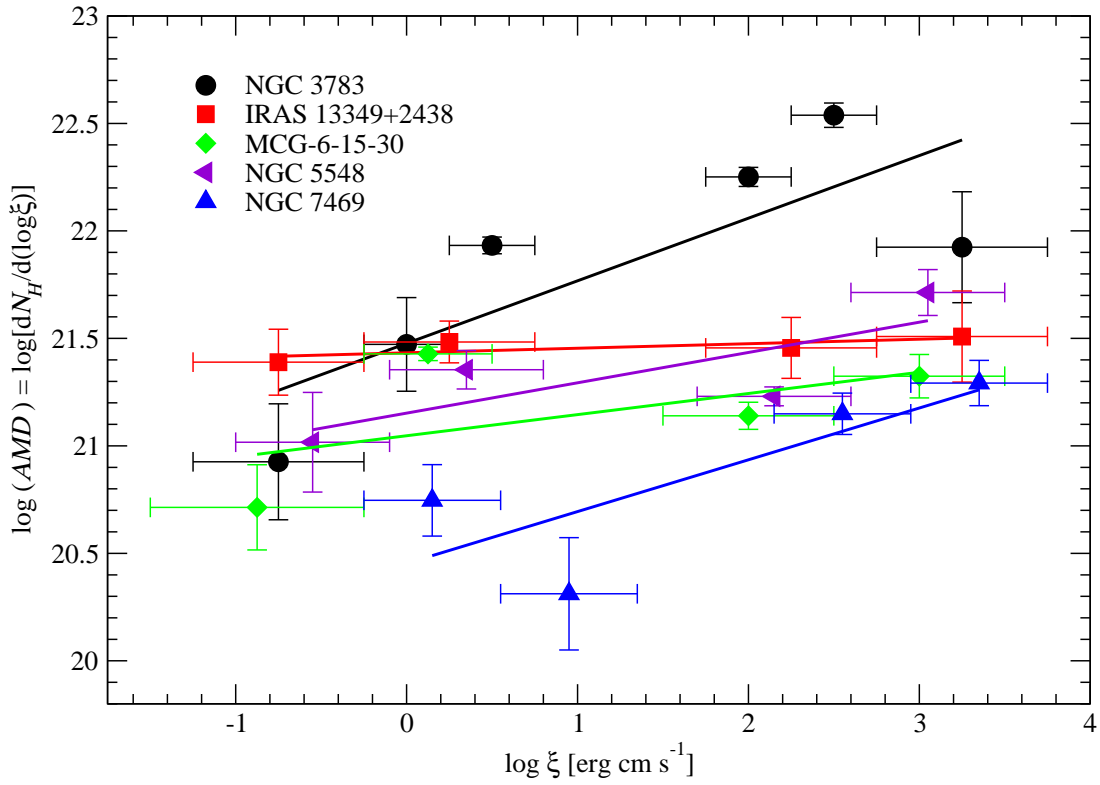


Fig. 1.— *AMD* distributions obtained for five targets. The best fit power-law is presented for each *AMD*. The inferred power-law slopes are relatively moderate, indicating a rather flat distribution of column density with ionization parameter.